Back

IMPACT ANALYSIS OF HELMETS FOR IMPROVED VENTILATION WITH DEFORMABLE HEAD MODEL

Praveen Kumar Pinnoji, Puneet Mahajan
Transportation Research and Injury Prevention Programme
Indian Institute of Technology Delhi, India

ABSTRACT

Wearing helmet in hot-humid climate is extremely uncomfortable due to excessive sweating. To enhance the evaporation of sweat alternative designs of the helmet are investigated. CFD simulations were performed in FLUENT™ to determine the velocity of air flow in the proposed helmet models. The head was approximated by a hemisphere and cylinder at the bottom. The presence of grooves enhanced remarkably the air flow velocities around the top of the head. Frontal and side impact simulations at different velocities up to 10m.s^{-1} were performed with helmet and deformable head model in LS-DYNA™. Pressure and stresses in the brain were investigated and were found not to change significantly due to the presence of grooves in the helmet.

Keywords: Helmets, Deformable head model, Ventilation and Dynamics

HELMETS are widely used by two wheeler riders to protect their head during the accidents or falls. In South Asia, excessive sweating and resulting discomfort due to hot and humid weather conditions discourages motorcycle riders from using helmets unless it is mandatory by law. The space between the head and helmet is small and air velocities in this gap are also low; as a result the sweat is unable to evaporate making the driver uncomfortable. To enhance the evaporation, alternative designs of the helmet with 11mm wide grooves in the foam were considered. In first ventilation design, the helmet had only one groove in the central plane with 7mm deep. In second design, the helmet had three parallel grooves of (each separated by 28mm) 7mm deep. In third design, the helmet had three parallel grooves cut through the foam thickness but not the shell. In the fourth design a 10 mm hole was provided in the shell of the third design. Computational fluid dynamics (CFD) simulations were performed with these helmet ventilation models to compare the air velocities with a conventional helmet. Front and side impact simulations for impact velocities up to 10m.s^{-1} were also performed to see if the presence of grooves has a detrimental effect on the dynamic performance of the helmet. In dynamic studies a deformable human head model was used. Head Injury Criterion (HIC), Von Mises stresses and Pressures were obtained in all these cases.

THERMAL DISCOMFORT AND VENTILATION

Due to excessive sweating while wearing a motorcycle helmet, people either avoid wearing a helmet or keep the straps loose so as to be able to wipe the sweat each time they stop on a crossing. A rough measure of the discomfort due to the wearing of helmet can be estimated by calculating the discomfort factor used in air conditioning (ASHRAE handbook). The human head was represented as two thermal compartments (or two node model) with inner one as body core and outer one as the skin layer. The total energy balance of the head can be represented as

Metabolic heat + Heat due to Sun = Sensible heat loss + Evaporative heat loss + Heat stored in the body

Metabolic rate and heat due to Sun on the head were taken as 6.7W/m^2 and 8.33W/m^2 which correspond approximately to 10% of total body values.

Energy balance on core yields,

$$M = (K + SKBF * c_{p,bl}) * (t_{cr} - t_{sk}) + m_{cr} * c_{cr} * \frac{dt_{cr}}{d\theta}$$

$$(K + SKBF * c_{p,bl}) * (t_{cr} - t_{sk}) + q_{sun} = q_{dry} + q_{evap} + m_{sk} * c_{sk} * \frac{dt_{sk}}{d\theta}$$

Energy balance for skin is,

$$t_{b,h} = \frac{0.347}{58.15} * (M - W) + 36.669$$

$$t_b = (1 - \alpha_{sk}) * t_{cr} + \alpha_{sk} * t_{sk}$$

Where,
M, Head metabolic rate = 6.7 W/m^2 (10% of total metabolic rate of the body)
K, Conductance between core and skin= 5.28 W/m^{2}k
SKBF, Blood flow rate in skin = ρ_{bl} x q_{bl} = 0.32 kg/hr.m^2
$C_{p,bl}$, specific heat of blood = 4190 J/kg.k
C_{cr}, specific heat of core = 3500 J/kg.k
C_{sk}, specific heat of skin = 3500 J/kg.k
q_{sun}, evaporative heat = 8.3 W/m^2
q_{dry}, sensible heat = (t_{sk} – 42) x 4.287 W/m^2
q_{evap}, evaporative heat = 61.2 W/m^2
W, rate of mechanical work done = 0.06 W/m^2
θ = time, sec
α_{sk} , fraction of the total body mass in the skin compartment = 0.042

The initial core temperature (t_{cr}) and skin temperatures (t_{sk}) were 36.8 ^{0}C and 33 ^{0}C respectively.

The discomfort factor, DISC, can be determined by

$$DISC = 4.7 * \eta_{evap} + 0.4685 * (t_b - t_{b,h})$$

Where,
η_{evap} is evaporative efficiency and assumed as 85%
t_b = mean body temperature and
$t_{b,h}$ = set point for evaporation in hot condition

According to AHSRAE handbook, discomfort can be defined on 0-5 grade scale, with grade 0 as comfortable and grade 5 as highly uncomfortable. From our thermal discomfort study, we obtained numerical value of 4.0 for DISC, with relative humidity 80%, which is highly uncomfortable while wearing helmet under hot and humid conditions. One of the ways to reduce the discomfort is to increase the evaporation rate of sweat by providing ventilation system in helmets for increased air velocities and thereby increased forced convection. Some possible ventilation models studied here, which provides grooves in the foam and a hole in the top of the outer shell. To visualize the fluid flow and velocity of air in the gap between the helmet and head in these ventilated helmet models computational fluid dynamics (CFD) simulations were performed. Some experiments in the wind tunnel on fluid flow in the gap between two hemispheres have also been performed for validation of velocities and pressures in numerical studies although these are not presented here. The convection coefficient due to increased velocities has not been calculated.

FLUID FLOW SIMULATIONS

The motion of fluids is described by the Navier-Stokes equations (NSEs), which are a set of coupled second order partial differential equations involving the variables p and u, which express the concepts of conservation of mass and momentum. The Navier-Stokes equations are obtained by combining these four equations [1988],

$$\dot{\rho} + \rho\left(\vec{\nabla} \cdot \mathbf{v}\right) = 0 \quad \text{(a)}$$

$$\vec{\nabla} \cdot \underset{\sim}{\mathbf{T}} + \rho\mathbf{b} = \rho\dot{\mathbf{v}} \quad \text{(b)}$$

$$\underset{\sim}{\mathbf{T}} = -p\underset{\sim}{\mathbf{I}} - \frac{2}{3}\mu\left(tr\underset{\sim}{\mathbf{D}}\right)\underset{\sim}{\mathbf{I}} + 2\mu\underset{\sim}{\mathbf{D}} \quad \text{(c)}$$

$$\underset{\sim}{\mathbf{D}} = \frac{1}{2}\left(\mathbf{v}\vec{\nabla} + \vec{\nabla}\mathbf{v}\right) \quad \text{(d)}$$

Where,
T = Fluid Stress tensor, ρ = density, v = velocity, D = Fluid Strain, p = pressure, b=gravity vector, μ = viscosity, I = Identity tensor, ∇ = the gradient operator, and *tr* denotes the trace of the indicated quantity

The time-derivative of the fluid velocity is defined as:

$$\frac{Dv}{Dt} = (\mathbf{v}.\nabla)\mathbf{v} + \frac{\partial v}{\partial t} \quad \text{(e)}$$

The Navier-Stokes equation for non-turbulent, Newtonian fluid obtained from above equations is

$$-\vec{\nabla}p + \mu\left(\vec{\nabla}^2\mathbf{v}\right) + \frac{1}{3}\mu\left(\vec{\nabla}\left(\vec{\nabla} \cdot \mathbf{v}\right)\right) + \rho\mathbf{b} = \rho\dot{\mathbf{v}} \quad \text{(f)}$$

$$-\vec{\nabla}p + \mu\left(\vec{\nabla}^2\mathbf{v}\right) + \rho\mathbf{b} = \rho\dot{\mathbf{v}} \quad \text{(g)}$$

Equation (f) is for compressible fluid and (g) is for incompressible fluid. The above equation can also be used to model turbulent flow, where the fluid parameters are interpreted as time-averaged values.

The NSE's are four equations for four unknowns and they are coupled, non-linear, and often involve complex geometries. For these reasons, it is rarely possible to find analytical solutions, and thus we must use computers to solve the equations. CFD numerical simulation packages such as FLUENT ™ use these equations to solve fluid motion in complex geometry more efficiently and effectively.

In fluid flow analysis, our main interest was to observe the changes in velocity in the gap of head and helmet if grooves were provided inside the helmet. Three-dimensional numerical simulations were done in FLUENT ™, by considering helmet as hemispherical and head as hemispherical with a cylinder (to represent the face) at the bottom. The gap between the head and helmet was 2 mm. Experiments were performed in the wind tunnel with a similar geometry but the gap between the head and helmet was 10 mm as accurate velocity measurements below this gap size were difficult. The results from the wind tunnel experiments were simulated using FLUENT ™ and a good match between experiments and simulations for pressure drops and velocities was obtained.

Figure 1 shows the helmet model with three parallel grooves. Figure 2 shows the meshed model of head and helmet in GAMBIT™ with a single groove and hole at the top. Inlet velocity of air was considered as 15m.s^{-1}. No-slip boundary conditions were assumed on the lower and upper walls and

out flow conditions were assumed at outlet. K-ε turbulent model is used for considering the viscous effects.

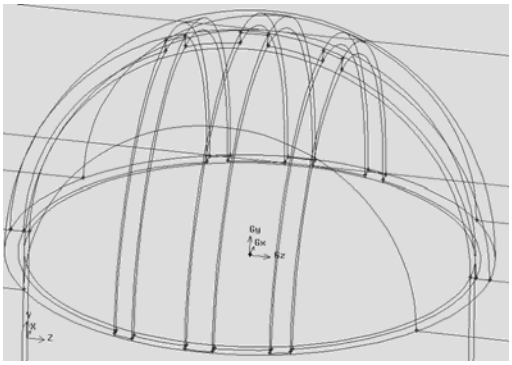

Fig.1 – Full view of 3-D helmet model with three parallel grooves

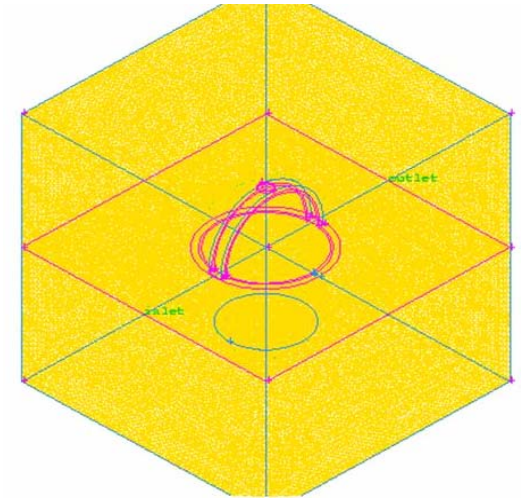

Fig.2 - Full view of 3-D meshed model with head and helmet with a groove in central plane

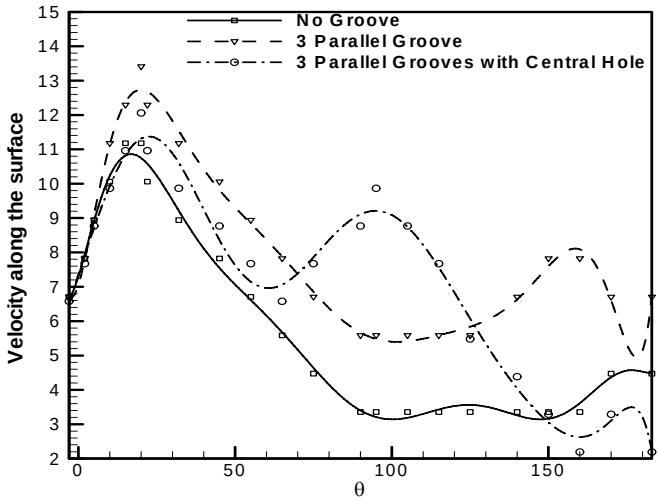

Fig.3 – Magnitudes of velocity in different grooved helmet models

Figure 3 compares velocities along the central plane of the head for foam with three grooves but shell without a hole, foam with grooves and shell with hole. Velocities (in m/s) along the gap were plotted on Y-axis and angle, θ (in degrees) along the X-axis. Grooves started at 0 degree and ended at 180 degrees along the circumference of the hemisphere. The presence of groove in the central plane raises the air velocity over the head in the grooved region by $2m.s^{-1}$. In case a hole is present in the shell the velocities next to the hole are high but drop rapidly thereafter and in the rear of the head below velocities are observed in absence of groove in the helmet. The velocities in the grooves on the sides showed a smaller increase in velocities as compared to the central plane. However, at the top of head improved velocity flows were also observed in the region between the central and side grooves.

DYNAMICS OF MOTORCYCLE HELMET

The dynamic performance of the ventilated helmet was studied using explicit Finite Element code LS-DYNA™. In the past the FE analysis of drop test of helmet used a rigid head and results were reported in the form of Head Injury Criterion (HIC) values and accelerations of the head form. Lately, FE is also commonly used to model the head [Horgan and Gilchrist 2003, Willinger et al. 2000 and Ruan et al. 1994]. Computed Tomography (CT) scanning and Magnetic Resonance Imaging (MRI) have been used to generate geometrical data in digital format for the head models. Once the geometry is available the material modeling of brain tissue is done next. Generally, the models do not contain all the details of the head and are much simpler than the actual head. One such 3D finite element model of human head developed by Willinger et al (2000) having skin, skull, CSF and brain is used here. The material properties of the various parts of the head were assumed to be homogeneous, isotropic and linearly elastic, except for the brain, which was assumed as viscoelastic in nature.

Initially, the frontal impact simulations were carried out at a velocity of $6.3m.s^{-1}$ with FE head model and a rigid sphere of 48mm radius. The pressure responses at coup and contra-coup are compared well with available literature. Horgan and Gilchrist (2003) and Zong et al. (2004) have also constructed three dimensional Finite element models of the human head. The former used it for simulating the pedestrian accidents whereas the latter authors use a SI (Structural Intensity) approach to study power flow distribution inside head in frontal, rear and side impacts. The results using human head models are presented in the form of pressures and stresses in the brain although a clear relation between stresses and brain injury are still to be fully established.

SHELL, FOAM AND HEAD – MATERIAL PROPERTIES

A motorcycle helmet has two major parts, namely, the outer shell and the energy absorbing liner, which we call as 'foam'. The energy absorbing liner is made of expanded polystyrene or EPS and outer shells are made from composite material, like fiberglass, carbon fiber and Kevlar, or a molded thermoplastic like ABS or polycarbonate. The outer shell resists the penetration of any foreign object and distributes the impact load on a wider area thus increasing the foam liner energy absorbing capacity. Material model 3 (*MAT_PLASTIC_KINEMATIC) available in LS-DYNA™ is used for outer shell in finite element analysis with following properties of Acrylo-Butadiene Styrene (ABS).

Table 1 - Material properties for Helmet shell

Part	Density ($kg.m^{-3}$)	Elastic Modulus ($N.m^{-2}$)	Yield stress ($N.m^{-2}$)	Poisson's ratio
Shell	2000	$1.7x10^{9}$	$34.3\ x10^{6}$	0.3

The liner considered here was manufactured from expanded polystyrene (EPS). Figure 4 shows the stress-strain behavior of EPS foam. The foam depicts linear elasticity at low stresses followed by a collapse plateau, truncated by a regime of densification in which the stress rises steeply. The longer

the plateau region more is the energy absorbed. Densification in the foam starts at 65% strain and stresses rise sharply after that.

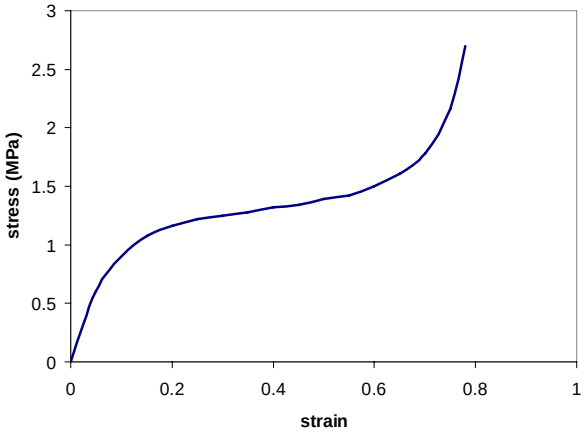

Fig.4 - Stress/Strain relationship for 44 kg.m^{-3} density of expanded polystyrene under quasi-static loading

Material model 63 (*MAT_CRUSHABLE_FOAM) available in LS-DYNA^{TM} was used for foam material. The model transforms the stresses into the principal stress space where the yield function is defined. If the principal stresses exceed the yield stress they are scaled back to the yield surface and transformed back to the original stress space. The yield surface and its evolution are defined by the equations:

Yield surface description:

$$f_t = |\sigma_i| - Y = 0$$

Hardening formulation:

$$Y = Y^0 + H(e_v)$$

$$Y_t = Y_t^0$$

where,
Y is the yield stress, Y^0 is initial compressive yield stress, Y_t is tensile cut off stress and σ_i is the principal stresses and H is strain hardening.

Here e_v is the volumetric strain defined by natural logarithm of relative volume. An associative flow rule is assumed and the plastic strains are derived from

Flow of plastic strains:

$$\dot{\varepsilon}_{ij}^{p} = \dot{\lambda}\frac{\partial F}{\partial \sigma_{ij}}$$

The flow surface is same as the yield surface.

In LS-DYNA^{TM} the data for stress versus volumetric strain for the liner are given in tabular form and it fits the above equations to this curve. The stress-strain curves, for three different densities of liner, for uni-axial loading are taken from Yettram [1994].

The various layers of the head like other biological materials do not follow the constitutive relations for common engineering materials and they are generally non-homogeneous, anisotropic, non-linear and viscoelastic. However, for modeling purposes here, they are assumed as homogeneous, isotropic and linearly elastic, except for the brain, which is assumed as viscoelastic in nature. The shear characteristics of viscoelastic behaviour of the brain are expressed by

$$G(t) = G_\infty + (G_0 - G_\infty)e^{-\beta t}$$

Here G_∞ is the long term shear modulus, G_0 is the short term shear modulus and β is the decay factor.
In the FE model of head of Willinger et al (2000), CSF was modeled as solid. Here it has been modified and modeled CSF as fluid in order to obtain reasonable head impact response. Material model 1 (*MAT_ELASTIC_FLUID) of LS-DYNA™ is used to model fluid in impact analysis and the properties are shown in table.2.

Table 2 - Material properties of CSF

Part	Density ($kg.m^{-3}$)	Bulk modulus ($N.m^{-2}$)	Poisson ratio
CSF	1040	2.19×10^7	0.49

Table 3 - Material properties of head parts

Part	Density ($kg.m^{-3}$)	Young's modulus ($N.m^{-2}$)	Poisson's ratio
Cranium	1800	15.0×10^9	0.21
Skin	1200	16.7×10^6	0.42
Tentorium	1140	31.5×10^6	0.23
Face	3000	5.0×10^9	0.21
Falx	1140	31.5×10^6	0.23

Table 4 - Material properties of brain

Part	Density ($kg.m^{-3}$)	Bulk modulus ($N.m^{-2}$)	G0 ($N.m^{-2}$)	GI ($N.m^{-2}$)	β (s^{-1})
Brain	2000	1.125×10^9	49.0×10^{-9}	16.7×10^{-9}	145

FINITE ELEMENT MODEL

HELMET-HEAD IMPACT ANALYSIS

The Finite element models of head provided by Willinger et al (2000) was combined with a commercially available helmet to determine the reduction in force experienced by the head and intracranial pressures during impact due to the presence of helmet. The foam or liner in helmet was of variable thickness with 28mm on front portion, 32mm on side and 40mm on top. Outer ABS shell was of 3mm thick.
Finite element simulations were performed for frontal and side impact against a rigid surface at different velocities up to $10 m.s^{-1}$ for the combined helmet-head model in LS-DYNA™. The full motorcycle helmet model required input data like geometry, initial and boundary conditions, interface conditions and material properties. Surface-to-surface contact interactions were used between the head

and helmet and between the helmet and rigid surface to prevent interpenetration of these surfaces. Figure 5 shows FE models of the head with a helmet undergoing frontal impact and side impact with a flat rigid surface.

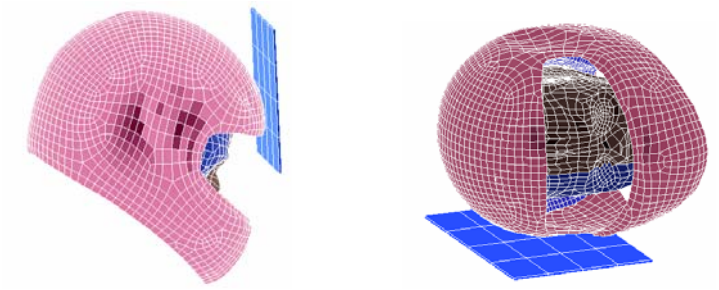

Fig.5 - Finite Element model of helmet-head in front and side impacts

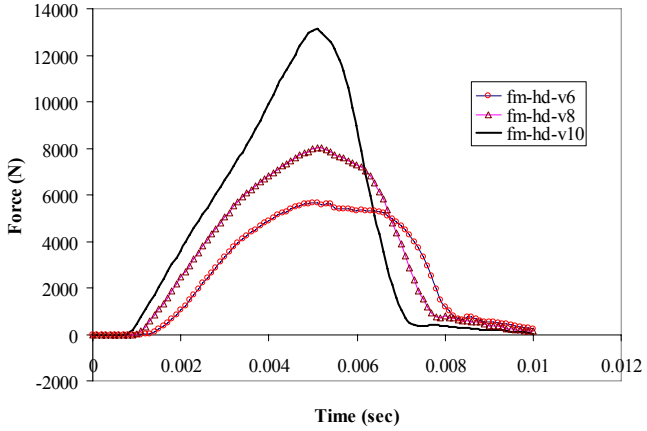

Fig.6 – Forces between helmet (no grooves) and head in front impact at 6, 8 and 10m.s^{-1} velocity

Figs.6 shows the contact forces between helmet and head for different velocities during the frontal impact. The maximum contact force for helmet without ventilation at 10m.s^{-1} velocity is 13000N; at 8m.s^{-1} velocity is 8000N and at 6m.s^{-1} velocity it is 5700N. The maximum force was reached at 5ms in all these cases. The foam in the impact region was completely bottomed out at 10 m.s^{-1} velocity. At 8 m.s^{-1} velocity, compression of foam was 80%; where as with 6 m.s^{-1} velocity it was 60% approx. Fig. 7 shows the contact forces experienced by the head at impact velocity of 6m.s^{-1} in helmet with single groove 7 mm deep, helmet with three grooves 7 mm deep and helmet with three grooves going through the thickness of the foam.

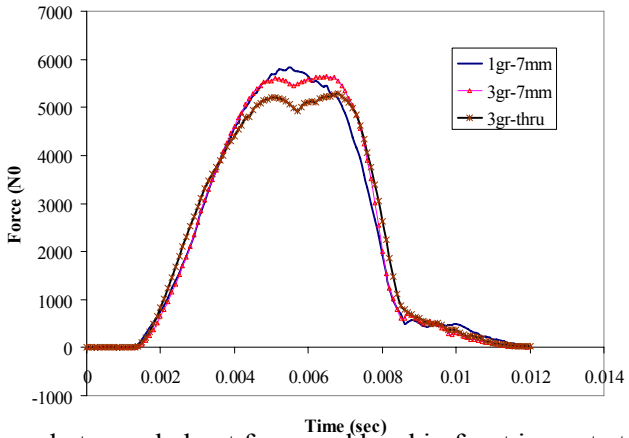

Fig.7 – Forces between helmet foam and head in front impact at 6m.s^{-1} velocity for different groove models

The contact force does not change appreciably when grooves do not run through the full thickness of the foam. In the helmet with three grooves of throughout the foam thickness the maximum contact force was lower at 5190N. This reduction is similar to what one observes with lower density foam except that no bottoming out of the foam occurs in the present case. The helmet impact duration is almost same in all these cases and is around 6.5ms. Similar results were obtained when the deformable head was replaced by a rigid head and HIC values, as shown in table 5, were calculated. The HIC value for the helmet with three parallel grooves throughout the foam thickness was the lowest at 848.

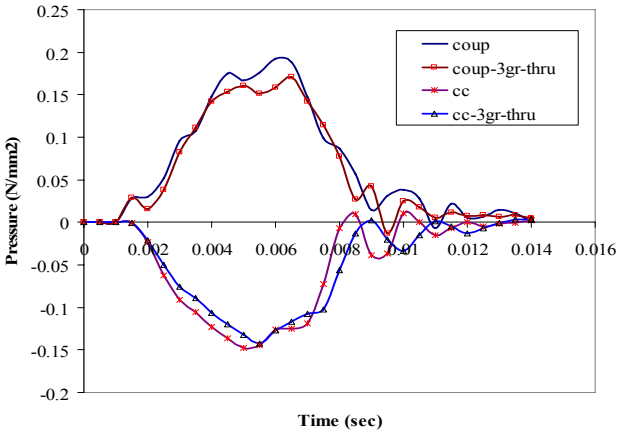

Fig.8 – Intracranial pressures in the front impact at 6m.s^{-1} velocity

Fig.8 compares intracranial pressures at coup and contra-coup sites. The trend of intracranial pressures at coup and contra-coup is similar in all the cases. With 7mm deep single groove or three grooves in the helmet, the value of pressure at coup site is 0.2MPa but with grooves going throughout thickness of foam the pressure is 0.17MPa. The pressures at contra-coup site are almost same in all the cases and they are of the range -0.14MPa.

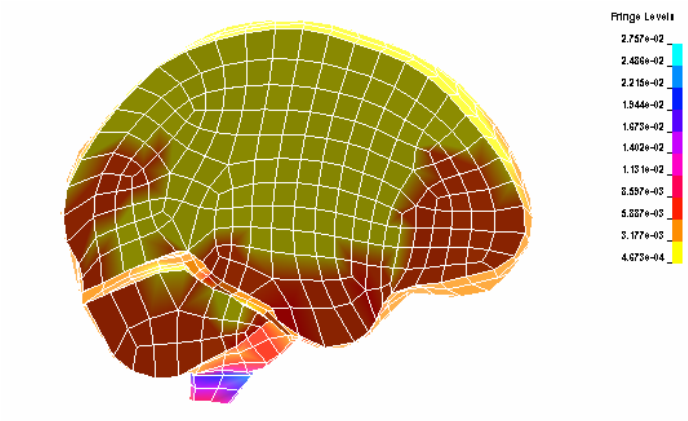

Fig.9 - Von Mises stresses in brain with three throughout the foam thickness grooves in helmet at time = 7.5ms

Stresses in the brain are slightly higher with helmet with no grooves and von Mises stresses are approximately 30.6kPa compared to other helmet models. Figure 9 shows the contours of von Mises stresses in the brain during the frontal impact of helmet with three grooves going through full thickness of the foam and a maximum value of 27.5kPa is reached in the brain stem at 7.5ms.

Table 5 -Head Injury Criterion (HIC) with different ventilation models

Helmet ventilation model	HIC
No grooves	977
One groove (7mm deep and 11mm width) in the central plane	999.2
Three parallel grooves (7mm deep and 11mm width)	975.5
Three parallel grooves (11mm width) with throughout foam thickness	848

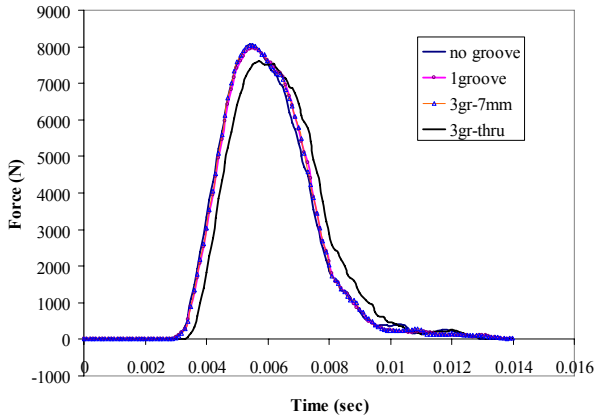

Fig.10 – Forces between helmet foam and head in side impact at 6m.s^{-1} velocity for different groove models

Figs.10 shows the contact forces between head and foam for different helmet models for side impact at 6m.s^{-1}. The behavior was similar to one seen in front impact. The contact force experienced by the head for a helmet with grooves through the thickness was 7600N as compared to 8000N experienced with other designs. The impact duration in side impact was same for all the cases and is 7ms.

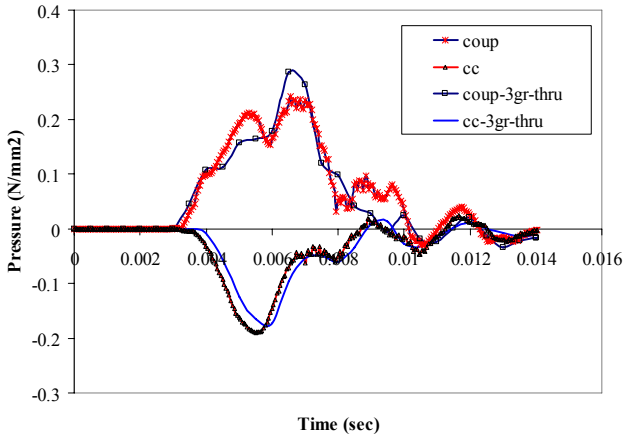

Fig.11 – Intracranial pressures in side impact at velocity 6m.s^{-1}

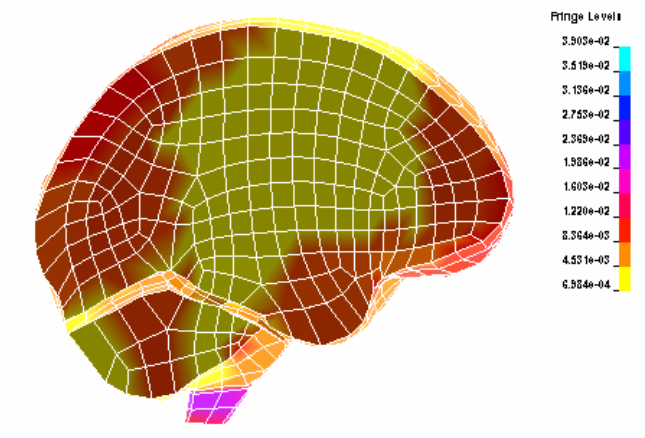

Fig.12 - Von Mises stresses in brain for side impact with three throughout the foam thickness grooves in helmet at time = 6.5ms

The intracranial pressures show a different behavior in side impact as compared to front impact. As seen in figure 11 in a helmet without groove, the coup pressure is 0.23MPa. But in the helmet with three parallel through grooves in foam the pressure is 0.28MPa. At contra-coup site, the pressure is approximately -0.19MPs for all design except for three grooves through thickness foam, in which pressure is -0.17MPa.

CONCLUSIONS

Computational fluid dynamics simulations show that air flow velocities can be substantially improved by providing grooves in the polymer foam liner. This should help in improving evaporation of sweat by increasing the convective heat transfer. A hole at the top in the helmet improves velocity locally at top of the head but velocities at the back of the head are lowered. The helmet with three parallel grooves running through the thickness of foam gave lower contact forces, HIC value and stresses in the brain when compared to other ventilation designs. The frontal and side impact results indicate that provision of grooves in the foam is not detrimental to the dynamic performance of the helmet.

REFERENCES

1. *AHRAE Handbook, Fundamentals*, Atlanta, GA: Am.Soc.of Heating, Refrigeration and Air-Conditioning Engineers, Inc., 1993, pp.8.1 – 8.29
2. Bruhwiler P A, Heated, perspiring manikin headform for the measurement of headgear ventilation characteristics, *Measurement of Science and Technology*, Institute of Physics publishing, Vol.14, 2003, pp.217-227
3. Fox and McDonald, *Introduction to Fluid Mechanics*, John Wiley publishers, 1988
4. Gibson L.J and Ashby M.F, *Cellular solids-structural and properties*, Pergamon Press, New York, 1988
5. Gilchrist and Mills, Impact deformation of ABS and GRP motorcycle helmet shells, *Plastics, Rubber and Composites Processing and Applications*, Vol.21, No.3, 1994, pp.141-150
6. Hallquist J.O., LS-DYNA3D Theoretical Manual, LSTC Report 1018, 1994
7. Horgan T.J. and Gilchrist M.D, Influence of FE model variability in predicting brain motion and intracranial pressure changes in head impact simulations, *Int. J. of Crashworthiness*, Vol.9, No.4, 2004, pp.401-418
8. Hanssen, A.G. et al., Validation of constitutive models applicable to aluminium foams, Int.J.of Mechanical sciences, Vol.44, 2002, pp.359-406

9. Kai-Uwe Schmitt et al., *Trauma Biomechanics Introduction to Accidental Injury*, Springer-Verlag, Berlin, 2004
10. Landro et al, Deformation mechanisms and energy absorption of polystyrene foams for protective helmets, *Polymer testing*, Vol.21, 2002, pp.217-228
11. Mitchell, D., Convective heat transfer in man and other animals, *Heat loss from animals and man*, Butterworth Publishing, London, 59, 1974
12. Ruan et al, Dynamic response of the human head to impact by three-dimensional finite element analysis, *Journal of Biomechanics*, Transactions of ASME, Vol.116, 1994, pp.44-50
13. Sznitman Josue et al., Flow visualization of bicycle helmets for optimal ventilation design, *Proceedings of HT2005, ASME summer Heat Transfer conference*, HT2005-72751, July 17-22, San Francisco, California, USA, 2005
14. Willinger et al, Finite element modeling of skull fractures caused by direct impact, *Int. Journal of Crashworthiness*, Vol. 5, No.3, 2000, pp.249-258
15. Yettram and et al, Materials for motorcycle crash helmets – a finite element parametric study, *Plastics, Rubber and Composites Processing and Applications*, Vol.22, No.4, 1994, pp.215-221
16. Zhang Jun et al., Constitutive modeling of polymeric foam material subjected to dynamic crash loading, *Int. J. Impact Engineering*, Vol.21, No.5, 1998, pp.369-386
17. Zong Z., Lee H.P., Lu C., A three-dimensional human head finite element model and power flow in a human head subjected to impact loading, *J. of Biomechanics*, 2005

Back